Published in final edited form as:
Sci Transl Med. 2016 October 26; 8(362): 362ra142. doi:10.1126/scitranslmed.aaf5187.

The neural basis of perceived intensity in natural and artificial touch

Emily L. Graczyk[1], **Matthew A. Schiefer**[2], **Hannes P. Saal**[3], **Benoit P. Delhaye**[3], **Sliman J. Bensmaia**[3], and **Dustin J. Tyler**[1,2,*]

[1]Department of Biomedical Engineering, Case Western Reserve University, Cleveland, OH 44106, USA

[2]Louis Stokes Cleveland Veterans AffairsMedical Center, Cleveland, OH 44106, USA

[3]Department of Organismal Biology and Anatomy, University of Chicago, Chicago, IL 60637, USA

Abstract

Electrical stimulation of sensory nerves is a powerful tool for studying neural coding because it can activate neural populations in ways that natural stimulation cannot. Electrical stimulation of the nerve has also been used to restore sensation to patients who have suffered the loss of a limb. We have used long-term implanted electrical interfaces to elucidate the neural basis of perceived intensity in the sense of touch. To this end, we assessed the sensory correlates of neural firing rate and neuronal population recruitment independently by varying two parameters of nerve stimulation: pulse frequency and pulse width. Specifically, two amputees, chronically implanted with peripheral nerve electrodes, performed each of three psychophysical tasks—intensity discrimination, magnitude scaling, and intensity matching—in response to electrical stimulation of

*Corresponding author. dustin.tyler@case.edu.

SUPPLEMENTARY MATERIALS
www.sciencetranslationalmedicine.org/cgi/content/full/8/362/362ra142/DC1
Materials and Methods
Fig. S1. Matching protocol setup.
Fig. S2. Threshold search procedure.
Fig. S3. Detection threshold as a function of stimulation PF.
Fig. S4. The effect of adaptation on sensory thresholds.
Fig. S5. Charge above threshold determines perceived intensity.
Fig. S6. Projected fields perceived on the missing hand from single-channel stimulation.
Fig. S7. Recruitment of afferent fibers with increasing charge.
References (44–50)

Author contributions: E.L.G. designed the experiments, collected the data, analyzed the data, created the computational model, and wrote the manuscript. M.A.S. designed the experiments, collected the data, and advised on result interpretation. H.P.S. designed the experiments, analyzed the data, generated the figures, and advised on result interpretation. B.P.D. analyzed the data, generated the figures, and advised on result interpretation. S.J.B. designed the experiments, developed the sensory neuroscience theoretical framework for the result interpretation, and wrote the manuscript. D.J.T. supervised the study, developed the neural engineering theoretical framework for the result interpretations, and wrote the manuscript.

Competing interests: D.J.T. and the Case Western Reserve University have filed patents on the FINE electrode used in these studies: "Flat interface nerve electrode and a method for use" (US6456866) and "Nerve cuff for implantable electrode" (US8868211 and pending patent application US 14/450,769). D.J.T., M.A.S., the Case Western Reserve University, and the Cleveland Department of Veterans Affairs Medical Center have filed patents for patterned stimulation paradigms: "Methods of treating medical conditions by population based encoding of neural information" (PCT/US2013/075329 with national filings in the United States, Europe, Canada, Australia, and Japan) and "Patterned stimulation intensity for neural stimulation" (PCT/US2014/070435 with national filings due in December 2016).

Data and materials availability: Raw data will be made available through material transfer agreement upon request to D.J.T.

their somatosensory nerves. We found that stimulation pulse width and pulse frequency had systematic, cooperative effects on perceived tactile intensity and that the artificial tactile sensations could be reliably matched to skin indentations on the intact limb. We identified a quantity we termed the activation charge rate (ACR), derived from stimulation parameters, that predicted the magnitude of artificial tactile percepts across all testing conditions. On the basis of principles of nerve fiber recruitment, the ACR represents the total population spike count in the activated neural population. Our findings support the hypothesis that population spike count drives the magnitude of tactile percepts and indicate that sensory magnitude can be manipulated systematically by varying a single stimulation quantity.

INTRODUCTION

Electrical stimulation of sensory nerves is a powerful tool for investigating neural coding at the sensory periphery and provides a means to restore sensation for patients who have lost it. In the sense of touch, previous studies with intraneural microstimulation revealed that electrical stimulation of individual tactile afferent neurons produces sensations that vary predictably on the basis of nerve fiber type (1–3), which constituted a major advance in our understanding of the neural basis of touch. In the field of neuroengineering, studies with human subjects provided evidence that electrically induced tactile and proprioceptive percepts improve the dexterous use of prosthetic hands (4–9), can be stable for years (10), and foster embodiment of the prosthesis by the subjects (11).

The magnitude of a tactile stimulus is one of its most basic sensory dimensions, one that can be resolved independently of its sensory quality. Tactile stimuli that vary widely in their other properties—spanning simple skin indentations, skin vibrations, and textures—can all be judged on a single intensive continuum (12–15). However, the neural determinants of tactile magnitude have not been conclusively elucidated. Increasing the intensity of a stimulus applied to the skin, such as the pressure exerted on the skin or the amplitude of a skin vibration, has two consequences on the evoked neuronal response: (i) an increase in the firing rate of nerve fibers whose receptive fields (RFs) lie at the locus of mechanical stimulation and (ii) the recruitment (activation) of fibers with nearby RFs (12, 13, 16–18). The contributions of these two aspects of the neural response to perceived intensity cannot be disentangled using recordings of afferent responses to mechanical stimulation of the skin because they covary to a large extent (12). Electrical stimulation of the nerve allows us to assess the influence of each of these two aspects of the neural response on the determination of sensory magnitude because firing rate and recruitment can be manipulated approximately independently by varying the stimulation pulse frequency (PF) and the charge per pulse, respectively.

In the context of upper-limb neuroprostheses, manipulating sensory magnitude is an intuitive way to convey information about the pressure exerted on objects (4). Previous experiments with electrical stimulation of human nerves demonstrated that adjusting the PF or manipulating the pulse amplitude (PA) or pulse width (PW) to alter the charge per pulse changes the perceived magnitude of the stimulus (5, 6, 19–23). However, these experiments did not provide a principled understanding of how stimulation parameters affect sensory

magnitude or how many discriminable levels of intensity could be provided through a peripheral nerve interface.

Here, we used classical psychophysical methods to systematically probe the dependence of sensory magnitude on stimulation parameters in two amputees equipped with flat interface nerve electrodes (FINEs) or spiral cuffs implanted for more than 2 years on their median, ulnar, and radial nerves (Fig. 1) (5). We sought to (i) elucidate the neural basis of sensory magnitude and (ii) leverage this newfound understanding to develop sensory encoding algorithms for use in sensorized neuroprostheses. To this end, we first used a two-alternative forced-choice paradigm to investigate the discriminability of sensory percepts evoked with different stimulation regimens. Second, we used free magnitude estimation to characterize how the sensory magnitude varies as stimulation parameters change. Third, we used an intensity matching paradigm to compare the perceived intensity of artificial and natural tactile percepts. In all experiments, we varied both the PF and the charge per pulse to assess the effects of each of these parameters on shaping the evoked percept. Frequency and charge per pulse have different effects on nerve activation, allowing the separation of the rate of activation from the number of fibers activated. We expected that the pattern of dependence of sensory magnitude on stimulation parameters would shed light on the neural basis of touch. We found that perceived intensity could be predicted on the basis of a single stimulation parameter that combined the PF and charge per pulse. We then showed that this parameter, which we have called the activation charge rate (ACR), approximates the total spike rate evoked in the activated neuronal population.

RESULTS

Subjects reliably discriminated small increments of stimulation PW or PF

We can discern the level of pressure applied to our fingertips with high accuracy based on neural signals from the skin (24), which are critical to our ability to dexterously manipulate objects (25, 26). For upper-limb neuroprostheses to be clinically viable, it is not sufficient to acquire and interpret control signals to move the limb, for example, from descending fibers in the nerve or from the activation of residual muscles; sensory information about the pressure exerted on objects must also be conveyed. Without these sensory signals, the ability to manipulate objects will be severely compromised. One approach to intuitively convey information about pressure is to modulate the intensity of electrical stimulation according to the applied pressure, with greater pressure signaled by greater intensity (4–6). With this in mind, we first sought to establish how changes in stimulation intensity led to distinguishable percepts. We had subjects discriminate the perceived intensity of pairs of stimulation pulse trains that varied in PW, PF, or both. These experiments yielded psychometric functions relating discrimination performance to differences in stimulation intensity (PW, PF, or both). To the extent that small increments in either parameter are discriminable, a large number of intensity levels can be signaled to the subject via the neural interface.

Systematic changes in stimulation parameters yielded systematic changes in the perceived magnitude of the evoked percepts, as evidenced by smooth psychometric functions, which are similar to those found in intact sensory systems (Fig. 2A). The just-noticeable difference (JND) is defined as the change in a stimulation parameter that yields 75% correct

discrimination. The JND for PF was 16.5±1.6Hz (mean±SD) and 29.6±4.6 Hz at 50- and 100-Hz references, respectively. To compare discriminability across stimulation conditions, we computed the Weber fraction, which is the JND divided by the reference. The Weber fractions obtained at the two reference frequencies were 0.33 and 0.30; these were statistically indistinguishable (unpaired *t* test, $P = 0.61$; Fig. 2B, inset). The JND for PW was 6.7 ± 1.0 μs, yielding a Weber fraction of 0.05, which was significantly lower than Weber fractions obtained with changes in PF (unpaired *t* test, $P < 0.001$ for both PF JNDs). We also found that discriminability was higher when both PF and PW increased or decreased together than when either changed in isolation or when they changed in opposite directions (Fig. 2C).

Subjects perceived a wide range of intensity of artificially evoked sensation

Discrimination performance does not provide information about the range of elicited sensations. All pulse trains might have elicited percepts whose magnitude was only slightly different but reliably so. Achieving natural somatosensory feedback would require that the artificial sensation perceptions span a wide range of sensory magnitudes that matches the range experienced in everyday life through an intact limb. To test the breadth of evoked sensations, subjects were asked to provide judgments of perceived intensity across the range of safe and comfortable stimulation parameters in a free magnitude scaling paradigm (12, 16, 27). As expected, the perceived intensity increased because PW (Fig. 3, A and C) and PF (Fig. 3, B and D) increased over the range of values tested. Perceived magnitudes of artificial touch spanned a wide range, increasing about 10-fold from the lowest to the highest intensity tested. To compare across stimulation parameters, we examined the intensity as a function of the average stimulation current, which is defined as the total stimulation charge applied per second (in units of microamperes)

$$I_{\text{ave}} = (\text{PW} * \text{PA}) * \text{PF} \quad (1)$$

The perceived magnitude as a function of average current was different depending on the mode of stimulation (*t* test comparing regression slopes, all $P < 0.001$; Fig. 3E): slopes were steepest for PW, shallowest for PF, and intermediate for the combination of PF and PW.

Subjects matched artificial tactile percepts to natural tactile stimuli

Having established that varying pulse train parameters can elicit a large number of discriminable intensity percepts and that these percepts span a wide range of intensities, we sought to directly compare the magnitude of electrically evoked sensations to that of mechanically evoked ones. To this end, subjects were instructed to match mechanical skin indentations on their intact hand to electrical stimulation such that the sensory magnitude of the former matched that of the latter. This process was repeated for electrical stimuli that spanned the range of perceptible and comfortable PWs and PFs. We found that PW and PF were approximately linear functions of indentation depth matched for perceived magnitude (Fig. 4, A to D). The slopes of the functions obtained by varying PF and PW were consistent for each electrode contact but varied across contacts. Electrode contacts that yielded a high

slope for indentation depth versus PF also yielded a high slope for indentation depth versus PW($r = 0.96$; Fig. 4E). The slopes of the functions were likely affected by several factors, including mechanical sensitivity at the location of the indentation, which probably varied across skin locations, and electrical sensitivity of the stimulated fascicle, which varied according to its geometry and distance from the stimulating electrode (see Biophysical model of afferent recruitment in the Supplementary Materials). As was the case with the magnitude estimates, PW and PF had different effects on matched depths when stimulation was expressed in terms of the average stimulation current (I_{ave}) (t test comparing regression slopes, all $P < 0.001$).

Total neural population spike rate encodes perceived intensity

Having established that changes in PF and PW have similar, but not equivalent, effects on sensation magnitude, we explored the implications of our findings on the underlying neural code. To this end, we applied stimulation recruitment principles to understand how these parameters might shape the neuronal response. Specifically, we examined how changes in PF and PW affect the activated neural population. Increasing the PF of stimulation results in an increase in the firing rate of activated neurons with miminal influence on the number of fibers activated, whereas increasing PW results in recruitment of additional neurons while minimally affecting the firing rate of the activated fibers because each pulse is too short to evoke multiple spikes in a given fiber (28–30). Electrical stimulation allows us to vary population size (via PW) and population firing rate (via PF) independently, which is not possible with natural stimulation because these two factors generally covary with mechanical stimulation of the skin.

Previous studies involving paired neurophysiological and psychophysical experiments yielded two theories of the neural basis of perceived intensity (12). According to the “hot zone” hypothesis, the perceived intensity is determined by the spike count across the population of afferent neurons whose RFs are directly under the stimulus, weighted by fiber type (12, 31). According to the “population” hypothesis, the perceived intensity is determined by the spike count across the entire population of afferent neurons that is activated by the stimulus, again weighted by fiber type. These two hypotheses could not be disambiguated on the basis of neurophysiological responses from the nerve and psychophysical ratings of perceived magnitude, as measured in monkeys and humans, respectively.

Results from the present study provide evidence against the hot zone model of perceived intensity. According to the hot zone model, increasing the PF of stimulation increases the sensory magnitude by increasing the firing of neurons while miminally recruiting additional neurons. In contrast, increasing the PW recruits additional neurons while minimally affecting the firing rate and has little impact on perceived intensity. On the other hand, the population model of perceived intensity predicts that increases in both stimulation parameters should affect the perceived magnitude because they both modulate the total number of spikes elicited: one by increasing the spike rate of activated neurons and the other by recruiting more neurons. In other words, both temporal and spatial summation seem to play a role in shaping perceived intensity.

On the basis of the hypothesis that the population model could quantitatively account for the behavioral results, we derived an expression to estimate how the population firing rate evoked by electrical stimulation varied as a function of PW and PF (for detailed derivation, see Derivation of activation charge rate in the Supplementary Materials). This model was predicated upon three assumptions: single fascicle activation, monotonic fiber recruitment, and single action potential per stimulation pulse. First, we assumed that only one fascicle was activated by any given stimulus, an assumption that is supported by in vivo tests of FINEs in animals (32) and by the observation that, in these experiments, the spatial extent of the projected field was stable across stimulation parameters (see fig. S6). Second, the number of fibers that were activated within the fascicle was a smooth, monotonic function of PW. This assumption is supported by the observation that perceived magnitude increased smoothly with increases in PW across the range tested. Recruitment, the proportion of fibers in the fascicle that are activated by each pulse, can be described as a sigmoidal function of PW (Fig. 5A). Whereas the threshold and slope are expected to vary across electrodes depending on the distance between the electrode and the stimulated fascicle, the precise electrical properties of the interposed tissue, the layout of surrounding fascicles, and the cross-sectional area of the fascicle, among others, a sigmoid is a generic description of the recruitment function (33). We implemented a detailed biophysical model of the human median nerve and of the effects of electrical stimulation on recruitment, showing that simulated recruitment curves were well approximated by a sigmoid function (fig. S7). When the stimulation is above threshold and in the linear range of the sigmoid, the total number of fibers activated is well approximated by a linear function of the total charge per pulse above threshold. Third, we assumed that each pulse produced a single action potential in each activated fiber, given the short PWs (all ≤255 μs) (28).

To estimate the total population spike rate, the proportion of activated fibers was multiplied by the stimulus frequency to yield a quantity we termed ACR

$$\mathrm{ACR} = (Q - Q_{\mathrm{thresh}}) * \mathrm{PF} \quad (2)$$

Because the stimulation pulses are square, the charge (Q) is the product of PA and PW, and Q_{thresh} is the charge at perception threshold. According to this model, the population firing rate is approximately linear with ACR (Fig. 5B).

When the electrical stimuli were expressed in terms of ACR and accounting for the effects of adaptation (see Measuring and modeling threshold adaptation in the Supplementary Materials), the psychometric functions obtained in the discrimination experiment and the resulting Weber fractions were consistent across the stimulation paradigms (t test for each pair, $P = 0.61$, 0.25, and 0.61, respectively; Fig. 6A). That is, the discriminability of two electrical stimuli could be predicted on the basis of this metric regardless of which stimulation parameter was varied. Similarly, the magnitude scaling and indentation matching functions obtained when varying each of the two parameters (PW or PF) overlapped almost completely when expressed in terms of ACR (Fig. 6, B and C), and the slopes were highly consistent across tested conditions (Fig. 6, D and E, all $P > 0.05$, except Fig. 6D, leftmost

panel, $P = 0.0059$). In other words, the perceived magnitude of any electrical stimulus could be predicted on the basis of ACR regardless of the specific stimulation parameters. Given that ACR is a proxy for the evoked population firing rate, the present results are consistent with the hypothesis that the perceived magnitude of a tactile stimulus is determined by the total firing rate evoked in the population of mechanoreceptive afferents innervating the skin.

DISCUSSION

A single code for perceived magnitude unifies natural and artificial touch

The intensity of a tactile percept is independent of its quality: different sensations can be evoked by different natural stimuli (for example, skin pressure and vibrations), but their intensity can be rated along a single continuum (12, 13). Here, we showed that the same applies to artificial touch: the intensity of electrically evoked percepts was determined by a single quantity, the ACR, although the quality of the evoked percept might vary across electrodes and even across stimulation regimes through a given electrode.

Increasing electrical input monotonically increases afferent activation

We did not directly test how fiber count increases with pulse charge because we could not measure fiber recruitment in these subjects. However, recruitment of motor neurons has been found to increase monotonically with pulse charge (34–37), and our biophysical model, based on measurements of human fascicle geometry, yielded a sigmoidal recruitment function (fig. S7). The stimulation paradigms tested here were likely operating in the approximately linear region between the threshold and saturation of this recruitment function. In these experiments, the term" threshold" refers to a perceptual threshold, not a single fiber activation threshold. With stimulation through an extraneural cuff, our results showed that even for near-threshold stimulation, the size of the projected field was larger than that of a single mechanoreceptive afferent (fig. S6), which implies that more than one afferent was recruited. It is also unlikely that we reached the saturation level because subjective magnitude did not plateau. Thus, for the stimulation paradigms tested here, the biophysical models predicted approximately linear recruitment with increases in pulse charge.

Sensory adaptation changes stimulation threshold

A ubiquitous phenomenon in sensory systems is that prolonged supra-threshold stimulation results in decreased sensitivity, as evidenced by increased detection thresholds and decreased sensory magnitudes. Although adaptation has been extensively documented with natural stimulation of the skin (38–42), less is known about its extent and time course with artificial electrical stimulation of the nerve. Here, we observed robust adaptation that depended systematically on the regimen of stimulation: stronger stimulation resulted in stronger desensitization. To estimate ACR, we therefore had to account for adaptation by adjusting the thresholds on a block-by-block basis according to the average stimulation strength of the previous block and the time between blocks. Although a systematic analysis of adaptation falls outside the purview of the present study, its effects will need to be taken into consideration when designing sensory feedback algorithms.

ACR simplifies the coding of intensity perception in neuroprostheses

The ability to systematically manipulate the perceived magnitude of an artificial tactile percept evoked through electrical stimulation of the nerve is critical for conveying meaningful information about contact events and for closed-loop control of upper-limb neuroprostheses (9). In particular, modulation of perceived magnitude can convey information about contact pressure (4). The output of pressure sensors can be converted into stimulation such that the sensory magnitude of the evoked percept is appropriate to the level of pressure applied (43). The key finding of the present study for the field of neuroprosthetics is that the effect of manipulations of PW and PF on perceived intensity can be systematically predicted on the basis of a single quantity, the ACR, which can be readily computed for any stimulation pulse train. Perceived magnitude could be predicted from this simple quantity in two subjects using three different approaches (intensity discrimination, magnitude estimation, and intensity matching). To scale perceived intensity, stimulation could vary in PF, PW, or both PF and PW. Because modulation of PF is predicted to affect the rate of axon firing but not the number of axons, PF is not expected to change the location and quality of the perception. Modulating PW is predicted to change the number of fibers activated and consequently may include concomitant changes in quality or location of sensation. Previous findings show that patterns of varied PW can change the quality of sensation (5). The results from this study suggested that PF could be covaried to control ACR and hence intensity, independently of quality. Functionally, if the maximum PF is 500 Hz and the maximum pulse charge is 0.25 μC (the charge density limit for our electrodes), 20 intensity levels can be reliably discriminated from just above threshold to this maximum intensity. This wide dynamic range is predicted to considerably improve the dexterity of manual manipulation with actuated neuroprostheses.

Tactile intensity and quality are conveyed through separate neural codes

There is more to touch than magnitude. The quality of the sensation also conveys important information about the nature of a stimulus and its dynamics. Although sensation quality was not systematically tested in these experiments, subjects reported experiencing nonpainful tactile sensations, using words such as “pressure,” “tingling,” “vibration,” “tapping,” and “touch” when prompted to describe the sensations. We propose that, whereas sensory magnitude is determined by the amount of activity in the nerve, sensory quality is determined by the patterning of this activity. In a previous study, the quality of a percept evoked by electrical stimulation of the nerve could be changed by temporally modulating the stimulation and thereby changing the evoked spatiotemporal pattern of neuronal activation (5). Combining stimulation patterns for quality and ACR for intensity offers independent control of these two aspects of sensation. However, the parameters of the stimulation pattern that caused a natural quality of sensation were frequency-dependent. The interaction of stimulation parameters on the various aspects of sensation will require more complex mapping algorithms and more complex stimulation patterns.

Because of the limits of the stimulation hardware, the effect of PA modulation on sensation intensity, rather than PW modulation, was not directly tested. The dependence of intensity on ACR is thus not known for PA modulation of the recruited neural population, but the results are expected to be similar to those shown here. Sensation intensity was only tested

for independent locations of perception. However, the subjects can feel and distinguish simultaneous sensations at multiple points on the hand. The ability to distinguish independent levels of sensation and interactions that might arise from multiple simultaneous sensations remains to be examined. The next big challenge in somatosensory neuroprostheses is to determine how to evoke sensations with predetermined qualities and graded intensities by evoking appropriate patterns of peripheral nerve activation while concurrently controlling ACR during electrical stimulation (4).

MATERIALS AND METHODS

Study design

The goal of this study was to determine how stimulation PW and PF affect the perceived intensity of artificial tactile percepts evoked through electrical stimulation. Tactile intensity was assessed in seven electrode contacts in two upper-limb amputee volunteers in a series of forced-choice tasks for intensity discrimination, perceived magnitude rating, and artificial-to-natural sensation matching. The data were used to create a model of the neural basis of perceived intensity. All experiments were double-blinded with randomized stimulus presentation order. A computer program controlled the stimulation, and raw data were analyzed by custom programs.

Subject inclusion criteria included unilateral, upper-limb amputees, aged 21 or older, who are current users of a myoelectric prosthesis or prescribed to use one and have viable target nerves in the residual limb. Potential subjects were excluded because of poor health (uncontrolled diabetes, chronic skin ulceration, history of uncontrolled infection, and active infection) or the presence of significant, uncontrolled persistent pain in the residual or phantom limb.

Subjects

Two male unilateral right-arm transradial amputees were implanted with FINEs or Case Western Reserve University (CWRU) spiral cuffs around their median, ulnar, and radial nerves in their residual limbs [see (5) for a complete description of the subjects and implants]. Briefly, subject 1 had a right transradial amputation just proximal to the wrist in 2010 due to a traumatic injury and was implanted in May 2012 with eight-contact FINEs around his right median and ulnar nerves and a four-contact CWRU spiral cuff around his right radial nerve. Subject 2 had a right transradial amputation in 2004 due to a traumatic injury and was implanted in January 2013 with eight-contact FINEs around his median, ulnar, and radial nerves. The present study was carried out between months 32 and 40 after implant for subject 1 and months 26 and 32 after implant for subject 2. The subjects visited the laboratory for 6-hour testing sessions every 2 to 6 weeks, depending on their availability. In referring to electrodes in the figures, we have adopted the convention E*x.y*, where *x* denotes the subject (1 or 2) and *y* denotes the electrode for that subject (ranging from 1 to 7). All study devices and procedures were reviewed and governed by the U.S. Food and Drug Administration Investigational Device Exemption, the Cleveland Department of Veterans Affairs Medical Center Institutional Review Board, and the Department of the Navy Human Research Protection Program. Informed consent was obtained from both subjects.

Peripheral nerve stimulation

All electrical stimuli consisted of trains of charge-balanced, square-wave, biphasic pulses with cathodal phase leading delivered by a custom Universal External Control Unit (Cleveland Functional Electrical Stimulation Center) stimulator to a single contact in the median nerve cuff (Fig. 1). The electrical returns consisted of one to three other contacts in the cuff such that stimulation elicited sensations on the palmar surface of the hand and did not interfere with the control of the myoelectric prosthesis. On each testing day, we obtained the subject's threshold on each cathodic contact using a two-alternative forced-choice tracking paradigm in two stages, focusing on the long-PW portion of the strength-duration curve. In stage 1, we found the PA threshold: on each trial, stimuli consisted of 5-s-long pulse trains at a PF of 100 Hz and a PW of 255 μs, which is the largest PW achievable with the stimulator, and the subject reported if the stimulus was perceived. PA started at 0.3 mA and was increased by 0.1 mA until the subject reported a sensation. In stage 2, we found the PW threshold: PA was held at threshold, PW started at 130 μs and, on each trial, was decreased by $130/2^n$ (where n is the number of reversals) when the subject reported sensation or increased by $130/2^n$ when the subject did not. Threshold was assumed once the PW step size became less than 5 μs (fig. S2).

Once the threshold was obtained, PW was increased in small steps to determine the range of parameters that led to sensations without causing discomfort. The midpoint of the range of PWs that elicited sensations was then selected as the set point PW for all subsequent discrimination trials. Similarly, stimuli at a range of PFs (at the set point PW)were presented to ensure that stimuli were perceptible and comfortable. The location, intensity, and quality of the sensations were recorded for several stimuli that spanned the range of PWs and PFs used in the discrimination experiments (described below). The quality of sensations tended to remain constant over the range of parameters tested.

Intensity discrimination

On each trial, two stimuli were presented, and the subject's task was to indicate which of the two was more intense (Fig. 2). Each experimental block comprised 180 trials, and the subjects were given a break between blocks. In each block, each stimulus pair was presented 20 times, and both the order of stimuli within the pair and the order of the pairs were varied pseudorandomly. The two pulse trains lasted 1 s and were separated by a 1-s interstimulus interval. The subject was instructed to ignore any changes in quality, duration, or location of the sensations if such changes were to occur and to focus solely on the intensity or magnitude of the sensation. Both the subject and the experimenter were blinded to the particular stimulation conditions of each trial. Discrimination data were fit with cumulative normal distributions to obtain psychometric functions. The JND was estimated as the change in the stimulation parameter (PF or PW)that yielded 75% correct performance. Each function yielded two estimates of the JND (one for decreases and the other for increases in that parameter relative to the reference parameter value), which were then averaged.

PF discrimination—Stimuli in each pair differed only in PF, with PA and PW held constant at their set point values, as described above. Each pair consisted of a stimulus at a reference PF, and the other was at a test PF. Two reference PFs—50 and 100 Hz—were

tested, and for each reference, the test PFs ranged from 25 to 175% of the reference PF with the following caveat: because the stimulator could only produce frequencies that were integer millisecond divisions of 1 s (that is, $f = 1/1$ ms, 1/2 ms, 1/3 ms, etc.), the nearest frequencies to achieve these reference percentages were used. Thus, for the 100-Hz reference, the test stimuli were 25, 50, 83.3, 90.91, 100, 111.1, 125, 142.9, and 166.7 Hz, and for the 50-Hz reference, the test stimuli were 12.5, 25, 40, 45.5, 50, 55.6, 62.5, 76.9, and 90.9 Hz.

PW discrimination—Stimuli in each pair differed in PW, with PF held constant at 100Hz and PAat its set value. One stimulus in each pair was the reference stimulus, where the PW was the set value used in the frequency discrimination trials. The other stimulus in the pair was the test stimulus, with PW typically ranging from 75 to 125% of the reference PW.

PF and PW discrimination—Stimuli in each pair differed in PW, PF, or both. One stimulus in the pair was always the reference stimulus, in which the PF and PW were at their set point values. This reference stimulus was compared to nine test stimuli that included every possible permutation of PF, which took on one of three values (at the reference level, below it, or above it), paired with a PW, which also took on one of these three values. The high and low values were selected based on previous trials to be slightly greater than or less than one JND (estimated from the PF and PW discrimination functions), respectively. For example, the PFs for subject 1 were 83.3, 100, and 125 Hz because the PF JND was found to be about 24 Hz on this contact, and the PWs were 121, 130, and 139 μs because the PW JND was found to be about 10 μs on this contact.

Magnitude estimation

On each trial, a 1-s-long pulse train was delivered, and the subject's task was to state a number whose magnitude corresponded to the magnitude of the evoked sensation. If a stimulus was imperceptible, it was ascribed the number 0. If one stimulus felt twice as intense as another, it was given a number that was twice as large. Subjects were encouraged to use fractions and decimals as needed, and there was not a maximum value. Trials were separated by at least 3 s to minimize adaptation (see the Supplementary Materials for the analysis of effects of adaptation). Subjects performed four experimental blocks, each consisting of 67 trials and being separated by breaks. Ratings were normalized by dividing the values by the grand mean rating on their respective blocks. In some cases, only three blocks were run because of time constraints.

The following three conditions were intermixed in a pseudorandom order in each experimental block: (i) in PF manipulation, the PW was constant at the reference PW, and the PF varied over a range from 25 to 166 Hz to be consistent with the discrimination and matching experiments; (ii) in PW manipulation, PF was constant at 100 Hz, and the PW varied along the perceptible and comfortable range; (iii) in PF and PW manipulation, the PF and PW spanned the same ranges as the PF and PW manipulations but increased together.

Electrical-to-mechanical intensity matching

Indentation stimuli were applied with micron precision (±2 μm) using a stage driven by an MX80LP servo motor with a 0.5-μm encoder (Parker Hannifin Corp.) (fig. S1). The motor was controlled by a ViX250IH servo driver (Parker Hannifin Corp.) under computer control using custom software. The stage was mounted on a stable frame constructed from extruded aluminum rods. On each experimental block, the indenter was positioned over the (intact) left hand, with the tactor centered on the location that matched the projected location of the sensations evoked when stimulating through the contact tested on that experimental block. The skin was preindented by ~500 μm to ensure that the tactor maintained contact with the skin over the entire block. Each trial consisted of a mechanical stimulus delivered to the intact hand paired with an electrical stimulus delivered through a given contact. Each stimulus lasted for 1 s and was separated by a 1-s interstimulus interval, followed by a response interval. The order of presentation of the stimuli (electrical or mechanical first) was randomized. The subject indicated which stimulus (mechanical or electrical) felt stronger. Each experimental block was divided into subblocks during which the electrical stimulus remained constant. Within each subblock, the depth of mechanical indentation increased (decreased) with a step size of 2 dB if the mechanical stimulus on the previous trial had been perceived as more (less) intense. In experiments with subject 1, the step size decreased from 2 to 0.25 dB after the first reversal, and the subblock ended after the second reversal. In experiments with subject 2, each subblock ended as soon as the subject's response reversed. In all experiments, the starting indentation depth was randomly selected to span the range of achievable depths. Each electrical stimulus was presented in five subblocks; subblocks with different electrical stimuli were interleaved in pseudorandom order. In PF manipulation, nine PFs were selected to span the range tested in the PF discrimination task (12 to 166 Hz). In PW manipulation, seven PWs were selected to span a range that was both perceptible and comfortable.

Statistical analysis

All data were reported as mean ± SD. Student's t test with $\alpha = 0.05$ was used for comparisons between stimulation conditions.

Supplementary Material

Refer to Web version on PubMed Central for supplementary material.

Acknowledgments

We thank M. Schmitt for clinical management of the subjects, as primary liaison to the local institutional review board, and for management of the study records. We thank M. Keith and J. R. Anderson for evaluation and primary medical responsibility for the subjects, surgical implementation of the system, and valuable clinical advice. We thank E. Schluter for the setup and operation of the sensitive testing apparatus required for the matching experiments. We thank D. Weber, Defense Advanced Research Projects Agency (DARPA) Hand Proprioception and Touch Interfaces (HAPTIX) program manager, for his support and thoughtful discussions during the performance of these experiments. We also thank the subjects for their patience and countless hours in the laboratory dedicated to improving the future of those with limb loss.

Funding: This work was sponsored by the DARPA Biological Technologies Office (BTO) HAPTIX program through the Space and Naval Warfare Systems Center (Pacific contract no. NC66001-15-C-4041), by the U.S. Department of Veterans Affairs Rehabilitation Research and Development Service Program (Merit Review Award

#I01 RX00133401 and Center #C3819C), by the NSF (grant no. DGE-1451075), and by the National Institute of Arthritis and Musculoskeletal and Skin Diseases (award number T32AR007505). The content is solely the responsibility of the authors and does not necessarily represent the official views of the listed funding institutions.

REFERENCES AND NOTES

1. Ochoa JL. Intraneural microstimulation in humans. Neurosci Lett. 2010; 470:162–167. [PubMed: 19818832]
2. Torebjörk HE, Schady W, Ochoa J. Sensory correlates of somatic afferent fibre activation. Hum Neurobiol. 1984; 3:15–20. [PubMed: 6330006]
3. Ochoa J, Torebjörk E. Sensations evoked by intraneural microstimulation of single mechanoreceptor units innervating the human hand. J Physiol. 1983; 342:633–654. [PubMed: 6631752]
4. Saal HP, Bensmaia SJ. Biomimetic approaches to bionic touch through a peripheral nerve interface. Neuropsychologia. 2015; 79:344–353. [PubMed: 26092769]
5. Tan DW, Schiefer MA, Keith MW, Anderson JR, Tyler J, Tyler DJ. A neural interface provides long-term stable natural touch perception. Sci Transl Med. 2014; 6:257ra138.
6. Dhillon GS, Horch KW. Direct neural sensory feedback and control of a prosthetic arm. IEEE Trans Neural Syst Rehabil Eng. 2005; 13:468–472. [PubMed: 16425828]
7. Raspopovic S, Capogrosso M, Petrini FM, Bonizzato M, Rigosa J, Di Pino G, Carpaneto J, Controzzi M, Boretius T, Fernandez E, Granata G, Oddo CM, Citi L, Ciancio AL, Cipriani C, Carrozza MC, Jensen W, Guglielmelli E, Stieglitz T, Rossini PM, Micera S. Restoring natural sensory feedback in real-time bidirectional hand prostheses. Sci Transl Med. 2014; 6:222ra19.
8. Clark GA, Wendelken S, Page DM, Davis T, Wark HAC, Normann RA, Warren DJ, Hutchinson DT. Using multiple high-count electrode arrays in human median and ulnar nerves to restore sensorimotor function after previous transradial amputation of the hand. Conf Proc IEEE Eng Med Biol Soc. 2014; 2014:1977–1980. [PubMed: 25570369]
9. Schiefer M, Tan D, Sidek SM, Tyler DJ. Sensory feedback by peripheral nerve stimulation improves task performance in individuals with upper limb loss using a myoelectric prosthesis. JNeural Eng. 2016; 13:016001. [PubMed: 26643802]
10. Tan DW, Schiefer MA, Keith MW, Anderson JR, Tyler DJ. Stability and selectivity of a chronic, multi-contact cuff electrode for sensory stimulation in a human amputee. JNeural Eng. 2015; 12:026002. [PubMed: 25627310]
11. Tyler DJ. Neural interfaces for somatosensory feedback: Bringing life to a prosthesis. Curr Opin Neurol. 2015; 28:574–581. [PubMed: 26544029]
12. Muniak MA, Ray S, Hsiao SS, Dammann JF, Bensmaia SJ. The neural coding of stimulus intensity: Linking the population response of mechanoreceptive afferents with psychophysical behavior. J Neurosci. 2007; 27:11687–11699. [PubMed: 17959811]
13. Poulos DA, Mei J, Horch KW, Tuckett RP, Wei JY, Cornwall MC, Burgess PR. The neural signal for the intensity of a tactile stimulus. J Neurosci. 1984; 4:2016–2024. [PubMed: 6470765]
14. Hollins M, Roy EA. Perceived intensity of vibrotactile stimuli: The role of mechanoreceptive channels. Somatosens Mot Res. 1996; 13:273–86. [PubMed: 9110430]
15. Talbot WH, Darian-Smith I, Kornhuber HH, Mountcastle VB. The sense of flutter-vibration: Comparison of the human capacity with response patterns of mechanoreceptive afferents from the monkey hand. J Neurophysiol. 1968; 31:301–334. [PubMed: 4972033]
16. Johnson KO. Reconstruction of population response to a vibratory stimulus in quickly adapting mechanoreceptive afferent fiber population innervating glabrous skin of the monkey. J Neurophysiol. 1974; 37:48–72. [PubMed: 4204567]
17. Mei J, Tuckett RP, Poulos DA, Horch KW, Wei JY, Burgess PR. The neural signal for skin indentation depth. II. Steady indentations. J Neurosci. 1983; 3:2652–2659. [PubMed: 6655504]
18. Burgess PR, Mei J, Tuckett RP, Horch KW, Ballinger CM, Poulos DA. The neural signal for skin indentation depth. I. Changing indentations. J Neurosci. 1983; 3:1572–1585. [PubMed: 6875657]
19. Anani AB, Ikeda K, Körner LM. Human ability to discriminate various parameters in afferent electrical nerve stimulation with particular reference to prostheses sensory feedback. Med Biol Eng Comput. 1977; 15:363–373. [PubMed: 197328]

20. Menia LL, van Doren CL. Independence of pitch and loudness of an electrocutaneous stimulus for sensory feedback. IEEE Trans Rehabil Eng. 1994; 2:197–206.
21. Dhillon GS, Krüger TB, Sandhu JS, Horch KW. Effects of short-term training on sensory and motor function in severed nerves of long-term human amputees. J Neurophysiol. 2005; 93:2625–2633. [PubMed: 15846000]
22. Szeto AY, Lyman J, Prior RE. Electrocutaneous pulse rate and pulse width psychometric functions for sensory communications. Hum Factors. 1979; 21:241–249. [PubMed: 489023]
23. Szeto AYJ. Relationship between pulse rate and pulse width for a constant-intensity level of electrocutaneous stimulation. Ann Biomed Eng. 1985; 13:373–383. [PubMed: 4073624]
24. Wheat HE, Salo LM, Goodwin AW. Human ability to scale and discriminate forces typical of those occurring during grasp and manipulation. J Neurosci. 2004; 24:3394–3401. [PubMed: 15056719]
25. Witney AG, Wing A, Thonnard JL, Smith AM. The cutaneous contribution to adaptive precision grip. Trends Neurosci. 2004; 27:637–643. [PubMed: 15374677]
26. Johansson RS, Flanagan JR. Coding and use of tactile signals from the fingertips in object manipulation tasks. Nat Rev Neurosci. 2009; 10:345–359. [PubMed: 19352402]
27. Stevens SS. The direct estimation of sensory magnitudes: Loudness. Am J Psychol. 1956; 69:1–25. [PubMed: 13302496]
28. McIntyre CC, Richardson AG, Grill WM. Modeling the excitability of mammalian nerve fibers: Influence of after potentials on the recovery cycle. J Neurophysiol. 2002; 87:995–1006. [PubMed: 11826063]
29. Grill WM, McIntyre CC. Extracellular excitation of central neurons: Implications for the mechanisms of deep brain stimulation. Thalamus Relat Syst. 2001; 1:269–277.
30. Yoshida K, Horch K. Selective stimulation of peripheral nerve fibers using dual intrafascicular electrodes. IEEE Trans Biomed Eng. 1993; 40:492–494. [PubMed: 8225338]
31. Bensmaia SJ. Tactile intensity and population codes. Behav Brain Res. 2008; 190:165–173. [PubMed: 18420286]
32. Tyler DJ, Durand DM. Functionally selective peripheral nerve stimulation with a flat interface nerve electrode. 2002; 10:294–303.
33. McIntyre CC, Grill WM. Finite element analysis of the current-density and electric field generated by metal microelectrodes. Ann Biomed Eng. 2001; 29:227–235. [PubMed: 11310784]
34. Gorman PH, Mortimer JT. The effect of stimulus parameters on the recruitment characteristics of direct nerve stimulation. IEEE Trans Biomed Eng. 1983; 30:407–414. [PubMed: 6604691]
35. Polasek KH, Hoyen HA, Keith MW, Tyler DJ. Human nerve stimulation thresholds and selectivity using a multi-contact nerve cuff electrode. IEEE Trans Neural Syst Rehabil Eng. 2007; 15:76–82. [PubMed: 17436879]
36. Polasek KH, Hoyen HA, Keith MW, Kirsch RF, Tyler DJ. Stimulation stability and selectivity of chronically implanted multicontact nerve cuff electrodes in the human upper extremity. IEEE Trans Neural Syst Rehabil Eng. 2009; 17:428–437. [PubMed: 19775987]
37. Crago PE, Peckham PH, Thrope GB. Modulation of muscle force by recruitment during intramuscular stimulation. IEEE Trans Biomed Eng. 1980; 27:679–684. [PubMed: 6970162]
38. Bensmaïa SJ, Leung YY, Hsiao SS, Johnson KO. Vibratory adaptation of cutaneous mechanoreceptive afferents. J Neurophysiol. 2005; 94:3023–3036. [PubMed: 16014802]
39. Leung YY, Bensmaïa SJ, Hsiao SS, Johnson KO. Time-course of vibratory adaptation and recovery in cutaneous mechanoreceptive afferents. J Neurophysiol. 2005; 94:3037–3045. [PubMed: 16222071]
40. Hollins M, Goble AK, Whitsel BL, Tommerdahl M. Time course and action spectrum of vibrotactile adaptation. Somatosens Mot Res. 1990; 7:205–221. [PubMed: 2378193]
41. Gescheider GA, Wright JH. Effects of sensory adaptation on the form of the psychophysical magnitude function for cutaneous vibration. J Exp Psychol. 1968; 77:308–313. [PubMed: 5655125]
42. Verrillo RT, Gescheider GA. Effect of prior stimulation on vibrotactile thresholds. Sens Processes. 1977; 1:292–300. [PubMed: 918678]

43. Tabot GA, Dammann JF, Berg JA, Tenore FV, Boback JL, Vogelstein RJ, Bensamaia SJ. Restoring the sense of touch with a prosthetic hand through a brain interface. Proc Natl Acad Sci USA. 2013; 110:18279–18284. [PubMed: 24127595]
44. Szeto AYJ, Saunders FA. Electrocutaneous stimulation for sensory communication in rehabilitation engineering. IEEE Trans Biomed Eng. 1982; 29:300–308. [PubMed: 7068167]
45. Kaczmarek KA, Webster JG, Bach-y-Rita P, Tompkins WJ. Electrotactile and vibrotactile displays for sensory substitution systems. IEEE Trans Biomed Eng. 1991; 38:1–16. [PubMed: 2026426]
46. Hollins M, Bensmaïa SJ, Washburn S. Vibrotactile adaptation impairs discrimination of fine, but not coarse, textures. Somatosens Mot Res. 2001; 18:253–262. [PubMed: 11794728]
47. Brill N, Tyler D. Optimizing nerve cuff stimulation of targeted regions through use of genetic algorithms. Conf Proc IEEE Eng Med Biol Soc. 2011; 2011:5811–5814. [PubMed: 22255661]
48. Swallow M. Fibre size and content of the anterior tibial nerve of the foot. J Neurol Neurosurg Psychiatry. 1966; 29:205–213. [PubMed: 5937634]
49. Verdú E, Ceballos D, Vilches JJ, Navarro X. Influence of aging on peripheral nerve function and regeneration. J Peripher Nerv Syst. 2000; 5:191–208. [PubMed: 11151980]
50. Peterson EJ, Izad O, Tyler DJ. Predicting myelinated axon activation using spatial characteristics of the extracellular field. J Neural Eng. 2011; 8:046030. [PubMed: 21750371]

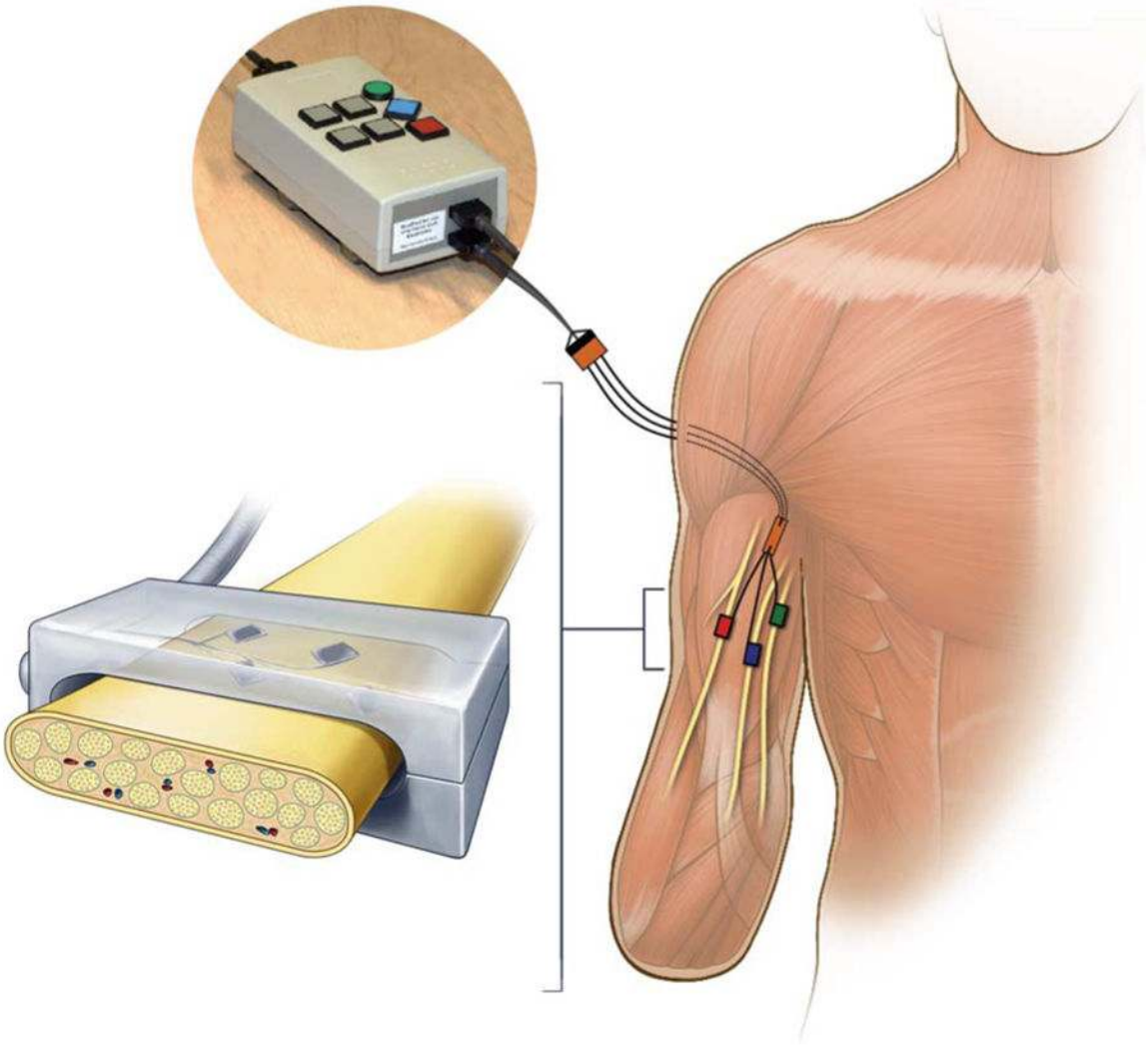

Fig. 1. Implanted peripheral nerve electrodes deliver stimulation directly to the nerve

Electrical stimulation was delivered by an external stimulator (top left) through percutaneous leads to FINEs implanted on the median, ulnar, and radial nerves of an upper-limb amputee (bottom left). Stimulation consists of trains of square, biphasic, charge-balanced pulses delivered to individual contacts in the eight-channel FINE. The FINE reshapes the nerve and achieves close proximity between the fascicles and the stimulating contacts, improving selectivity. Each electrode contact evokes sensory percepts on small regions of the missing hand of the subject.

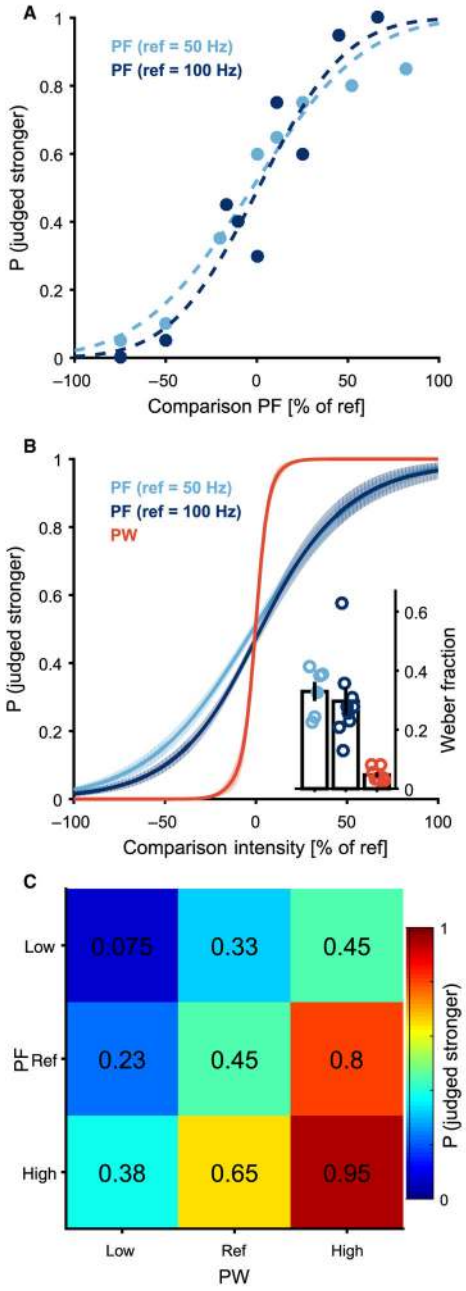

Fig. 2. Intensity discrimination performance yields smooth psychometric functions

(**A**) Discrimination performance as a function of comparison PF. Comparison PF is reported as a percentage of reference PF for one electrode E2.6 and two reference (ref) PFs, 50 and 100 Hz. Points indicate percentage of test stimuli correctly identified as stronger or weaker than the reference over 20 pairwise trials, and the dashed line is the sigmoidal fit to the raw data. (**B**) Combined discrimination curves from multiple electrode contacts across two subjects under three conditions (PF discrimination, 50-Hz reference, $n = 6$; PF discrimination, 100-Hz reference, $n = 7$; PW discrimination, $n = 7$) (solid line denotes the mean and shaded area denotes the SEM). (Inset) Weber fractions calculated as JND divided

by the reference value for the three conditions. Weber fractions were significantly lower for PW than either PF condition (*t* test, $P < 0.001$ for both) but did not differ between PF at 50 Hz and PF at 100 Hz (*t* test, $P = 0.61$). Open circles denote all data; bars denote the mean and SEM; filled circles correspond to curves in (A). (**C**) Intensity discrimination performance with variations of both PF and PW averaged across subjects ($n = 2$). Values indicate the percentage of times that a particular test stimulus was identified as stronger than the reference stimulus (center square). The reference was compared to nine test stimuli that varied in both PW and PF and included combinations of the following: lower than the reference PF level, at the reference PF level, and higher than the reference PF level; lower than the reference PW level, at the reference PW level, and higher than the reference PW level. The high and low PF and PW values were chosen to be slightly greater than or less than one JND, respectively, as determined by testing shown in (A) and (B). The stimulus with the highest PW and PF is in the lower right corner, and the stimulus with the lowest PW and PF is in the upper left. Whenever one or both of the parameters increased, the percentage of times the stimulus was judged stronger than the reference increased.

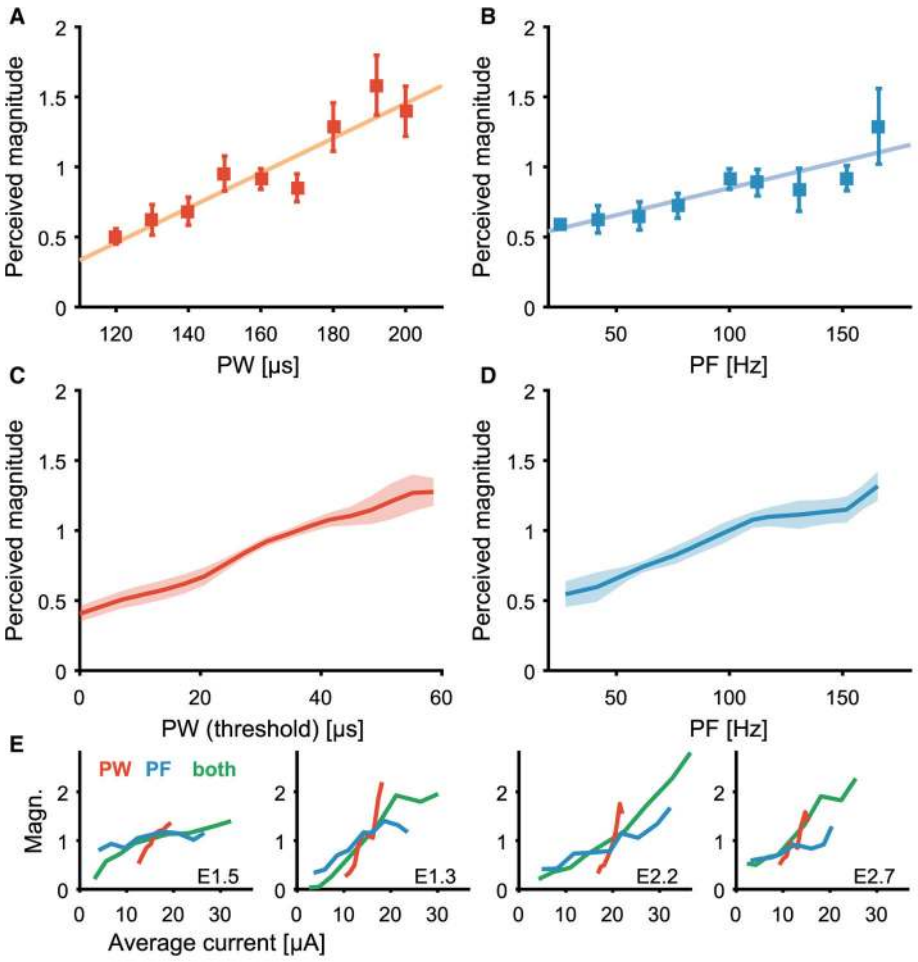

Fig. 3. Perceived magnitude scales with PW, PF, or both

(**A** and **B**) Normalized perceived magnitude as a function of PW(A) or PF (B) for one electrode (E2.7, all other stimulus parameters held constant). Points indicate mean ratings (n= 10); error bars denote the SEM; the colored line is the line of best fit. (**C** and **D**) Normalized perceived magnitude as a function of PW (C) or PF (D) averaged across electrodes (n = 4). Shaded areas denote the SEM. (**E**) Average normalized perceived magnitude as a function of average current for individual electrodes. Manipulations of PW (red), PF (blue), or PW and PF combined (green). Slopes were significantly different depending on stimulation condition (t test, $P < 0.001$).

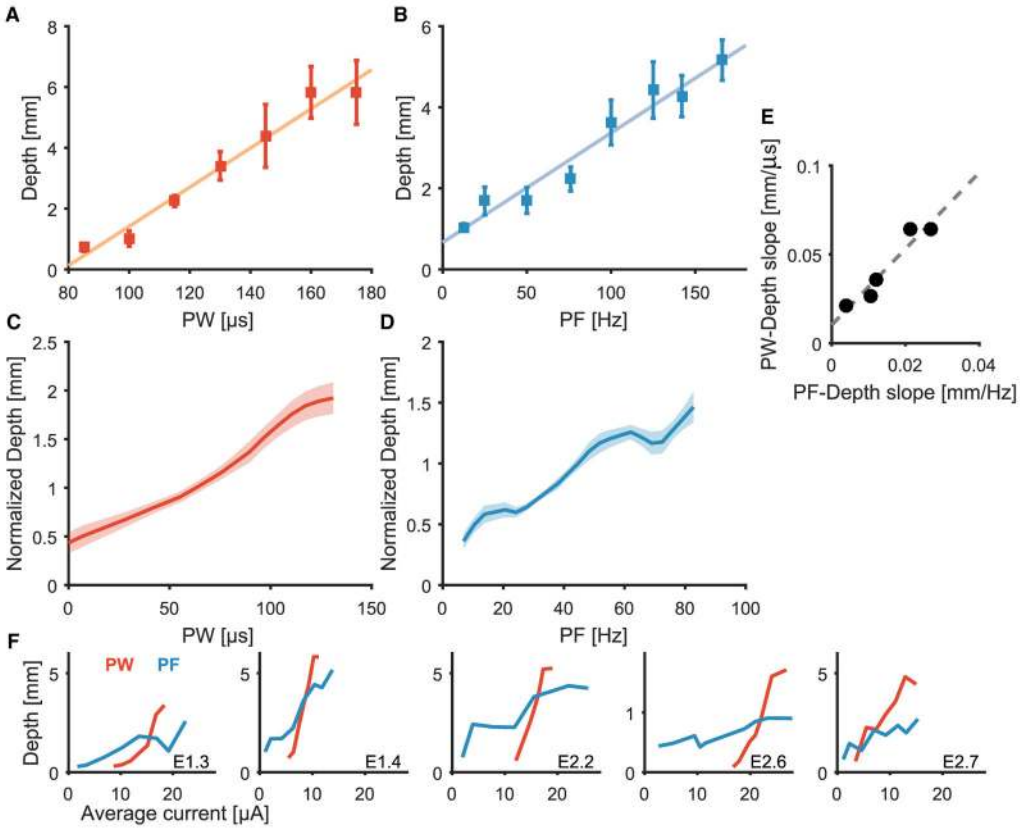

Fig. 4. Matching of fingertip indentations on the residual limb to electrical stimuli delivered to the contralateral nerve

(**A** and **B**) Indentation depth matched to PW (A) and PF (B) for one electrode (E2.2). Points indicate mean depths ($n = 5$); error bars denote SEM; the colored line is the line of best fit. (**C** and **D**) Normalized indentation depth matched to PW (C) or PF (D), averaged across subjects and electrode contacts ($n = 5$). Shaded areas denote SEM. (**E**) Relationship between PF and PW regression slopes for each electrode, where each point represents a different electrode contact ($n = 5$; correlation analysis, $r = 0.96$). (**F**) Indentation depth as a function of average current for each electrode when matched to PW (red) and PF (blue). PW and PF had significantly different effects on matched indentation depth (t test, $P < 0.001$).

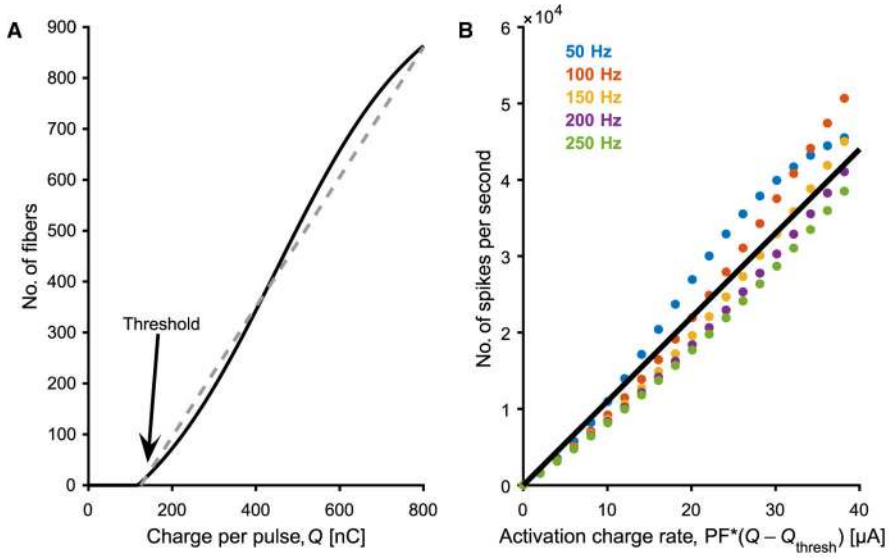

Fig. 5. Graphical representations of hypothesized neural response to stimulation intensity and spike frequency

(**A**) Recruitment of nerve fibers is hypothesized to increase with increased stimulation intensity (charge per pulse). Arrow indicates the putative location of the perceptual threshold. (**B**) Neural population firing rate as a function of ACR. Assuming each pulse produces one spike per activated fiber, this yields an approximately linear function. Threshold is assumed to be independent of PF (see fig. S3).

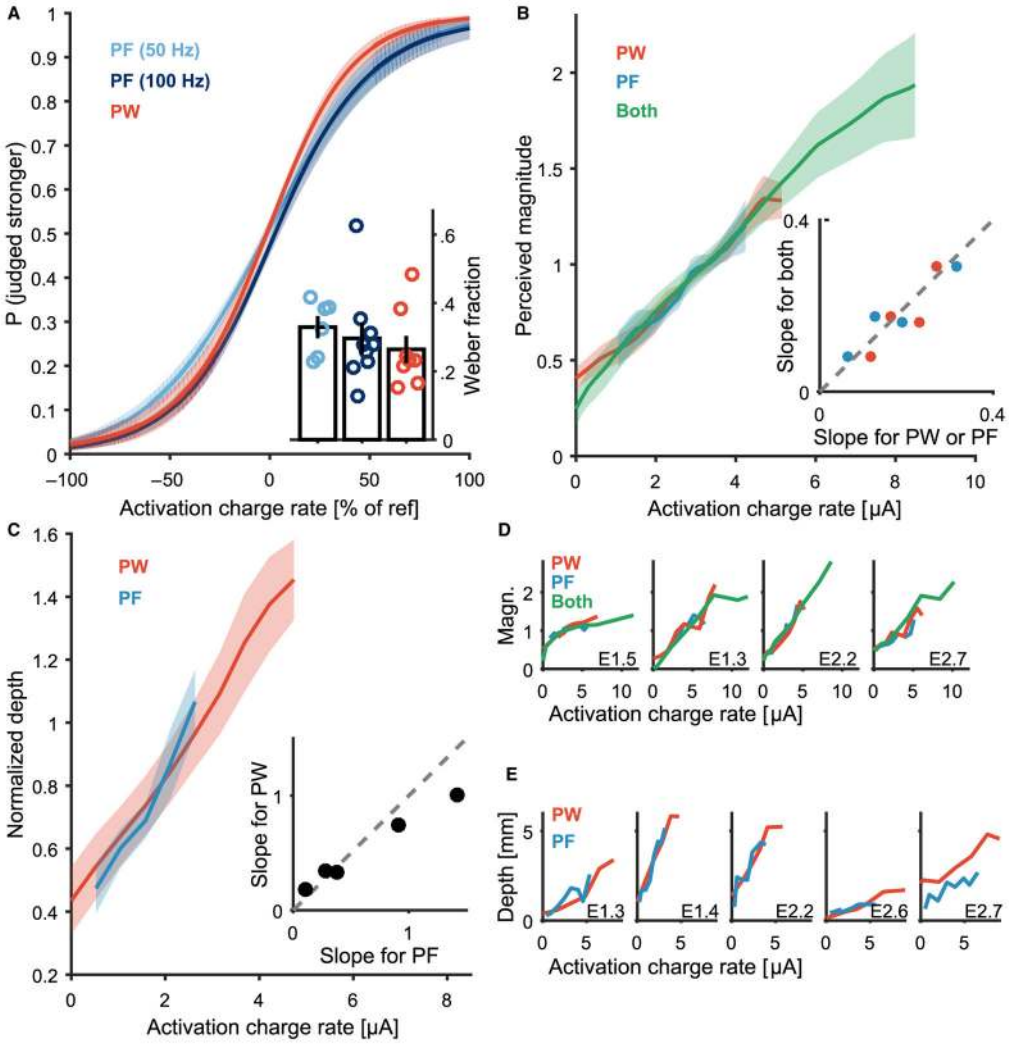

Fig. 6. ACR determines perceived intensity

(**A**) Intensity discrimination: performance as a function of ACR, accounting for adaptation (see figs. S4 and S5). (Inset) Weber fractions obtained from the three stimulation conditions: PW, PF at 50 Hz, and PF at 100 Hz. Weber fractions were consistent across the stimulation paradigms (*t* test, $P = 0.61$, 0.25, and 0.61). (**B**) Magnitude estimation: perceived intensity as a function of ACR for the PW, PF, and combined PF and PW manipulation, averaged across electrodes ($n = 4$). The shaded area denotes SEM. (Inset) Comparison of regression slopes obtained when varying PW, PF, or PW and PF for each electrode. Each blue point compares the slope of the PF manipulation to the slope of the combined PW and PF manipulation for a single electrode contact ($n = 4$). Each red point compares the slope of the PW manipulation to the slope of the combined PW and PF manipulation for a single electrode contact ($n = 4$). (**C**) Normalized indentation depth matched for perceived intensity as a function of ACR, averaged across electrodes ($n = 5$). Shaded area denotes SEM. (Inset) Comparison of regression slopes obtained when varying PF or PW for each electrode (n=5). (**D**)Magnitude estimates of intensity as a function of the ACR for the PW, PF, and combined PW and PF manipulation for each electrode. Slopes were consistent across stimulation conditions (*t* test,

$P > 0.05$ for all comparisons, except leftmost panel $P = 0.0059$). (**E**) Indentation depth matched for perceived intensity as a function of ACR for each electrode. Slopes were consistent across stimulation conditions (*t* test, $P > 0.05$ for all).